Cancer Research

Connexin 43 Inhibition Sensitizes Chemoresistant Glioblastoma Cells to Temozolomide

Susan F. Murphy[1], Robin T. Varghese[1], Samy Lamouille[1,2], Sujuan Guo[1], Kevin J. Pridham[1], Pratik Kanabur[1], Alyssa M. Osimani[1], Shaan Sharma[1], Jane Jourdan[1], Cara M. Rodgers[3], Gary R. Simonds[3], Robert G. Gourdie[1,4,5,6], and Zhi Sheng[1,4,7,8]

Abstract

Resistance of glioblastoma (GBM) to the front-line chemotherapeutic agent temozolomide (TMZ) continues to challenge GBM treatment efforts. The repair of TMZ-induced DNA damage by *O*-6-methylguanine-DNA methyltransferase (MGMT) confers one mechanism of TMZ resistance. Paradoxically, MGMT-deficient GBM patients survive longer despite still developing resistance to TMZ. Recent studies indicate that the gap junction protein connexin 43 (Cx43) renders GBM cells resistant to TMZ through its carboxyl terminus (CT). In this study, we report insights into how Cx43 promotes TMZ resistance. Cx43 levels were inversely correlated with TMZ sensitivity of GBM cells, including GBM stem cells. Moreover, Cx43 levels inversely correlated with patient survival, including as observed in MGMT-deficient GBM patients. Addition of the C-terminal peptide mimetic αCT1, a selective inhibitor of Cx43 channels, sensitized human MGMT-deficient and TMZ-resistant GBM cells to TMZ treatment. Moreover, combining αCT1 with TMZ-blocked AKT/mTOR signaling, induced autophagy and apoptosis in TMZ-resistant GBM cells. Our findings suggest that Cx43 may offer a biomarker to predict the survival of patients with MGMT-independent TMZ resistance and that combining a Cx43 inhibitor with TMZ could enhance therapeutic responses in GBM, and perhaps other TMZ-resistant cancers. *Cancer Res; 76(1); 139–49. ©2015 AACR.*

Introduction

In the central nervous system, glioblastoma (GBM) is the most common malignancy, accounting for more than 45% of all malignant brain tumors. The percentage of GBM patients with 5-year survival after aggressive treatment is less than 5%, ranking it the most lethal of all brain cancers and the sixth most deadly of all types of malignancy (1). Standard of care for newly diagnosed GBM includes maximum safe resection, followed by ionizing radiation and chemotherapy with temozolomide (TMZ). However, even after extensive and aggressive surgical resection of tumors, median survival is increased by only 2.5 months (from 12.1 to 14.6 months), with combined TMZ and radiation therapy (2). Before the addition of TMZ to standard of care in 2005, no improvement in survival from newly diagnosed GBM had been achieved in decades despite numerous clinical trials on various new treatments (3). The grim fact that an increase of only 2.5 months represents a significant improvement in survival for GBM patients highlights the urgent need for more efficacious treatments.

TMZ is a DNA-alkylating agent that causes lethal DNA lesions in fast-dividing cancer cells. This drug is widely used to treat primary, as well as metastatic brain cancer. However, substantial resistance typically develops to TMZ, and with this, the drug shows decreased clinical efficacy. Poor response to TMZ is often associated with *O*-6-methylguanine-DNA methyltransferase (MGMT), an enzyme that repairs damage to DNA induced by TMZ. Although a subset of patients without MGMT activity (often resulting from methylation of the MGMT promoter) shows better responsiveness to TMZ, relapse eventually develops (4). Thus, brain cancer patients exhibit MGMT-dependent and -independent patterns of resistance to TMZ. Although MGMT-dependent TMZ resistance is attributable to the presence of active MGMT, the mechanisms underlying MGMT-independent resistance remain to be elucidated. In addition, inhibiting MGMT failed to show clinical benefit for TMZ-refractory patients. Thus, new therapeutic strategies that improve response to TMZ treatment regimes could have a genuine impact on the clinical management of GBM.

Recently, a number of groups have reported several lines of evidence that the gap junction protein Cx43 (also called gap junction protein A1, *GJA1*) controls the response of GBM cells to TMZ (5–8). First, Cx43 was found to be highly expressed in GBM tissues compared with normal brain (7, 8). Second, overexpressing Cx43 in GBM cell lines rendered them resistant to TMZ (7, 8). Third, genetic knockdown of Cx43 or an antibody against Cx43 restored TMZ sensitivity (6–8). Finally, GBM cells expressing a CT truncation of Cx43 recovered sensitivity to TMZ (8). Collectively, these results indicate that pharmacologic targeting of Cx43 could help overcome TMZ resistance in some cell lines and tumors.

[1]Virginia Tech Carilion Research Institute, Roanoke, Virginia. [2]FirstString Research Inc., Mount Pleasant, South Carolina. [3]Department of Neurosurgery, Carilion Clinic, Roanoke, Virginia. [4]Faculty of Health Science, Virginia Tech, Blacksburg, Virginia. [5]Virginia Tech-Wake Forest University School of Biomedical Engineering and Sciences, Blacksburg, Virginia. [6]Department of Emergency Medicine, Virginia Tech Carilion School of Medicine, Roanoke, Virginia. [7]Department of Biological Sciences and Pathobiology, Virginia-Maryland College of Veterinary Medicine, Virginia Tech, Blacksburg, Virginia. [8]Department of Internal Medicine, Virginia Tech Carilion School of Medicine, Roanoke, Virginia.

Corresponding Authors: Zhi Sheng, Virginia Tech, 2 Riverside Circle, VA 24016. Phone: 540-526-2042, Fax: 540-985-3343; E-mail: zhisheng@vtc.vt.edu, and Robert G. Gourdie, E-mail: gourdier@vtc.vt.edu

doi: 10.1158/0008-5472.CAN-15-1286

We have developed a Cx43 C-terminus (CT) mimetic peptide-dubbed αCT1. αCT1 is a 25mer peptide comprising the ZO-1 PDZ-binding domain of Cx43 fused to an N-terminal antennapedia cell penetration sequence. This Cx43 CT mimetic was originally designed as a tool to disrupt the interaction between endogenous ZO-1 and Cx43 in studies of heart electrical conduction (9). Importantly, αCT1 has completed testing in phase II clinical trials as a wound-healing drug, with no treatment-associated adverse events found in the more than 250 patients that participated in these studies (10). In this report, we investigated the relationship between Cx43 and MGMT-independent TMZ resistance and patient survival. We also monitored the response of GBM to αCT1 and TMZ, determining that this combinatorial treatment results in a striking recovery in sensitivity to TMZ of human GBM cells and tumors.

Materials and Methods

Reagents

Reagents were as follows: αCT1 peptide was purchased from the American Peptide Company. Lyophilized peptide powder was reconstituted in 1× PBS (137 mmol/L NaCl, 2.7 mmol/L KCl, 10 mmol/L Na_2HPO_4, and 1.8 mmol/L KH_2PO_4) at a concentration of 5 mmol/L. The Cyto-ID dye was purchased from Enzo Life Sciences, Inc. TMZ was purchased from Selleck Chemicals LLC. TMZ was reconstituted in DMSO and then aliquots were stored at −20°C freezer. The stock concentration of TMZ is 50 mmol/L. Normal brain cell lysate was purchased from Abcam.

GBM cell lines

Human GBM cell lines SF295, U87MG, A172, LN229, T98G, SF-268, U251, SNB-75, LN-18 were maintained in DMEM (Life Technologies Corporation) supplemented with 10% FBS (Atlas Biologicals, Inc.), streptomycin (100 μg/mL), and penicillin (100 IU/mL). Human GBM stem cell (GSC) lines LN229/GSC and GS9-6/NOTCH1+ cells were maintained as spheres in Neuralbasal media (Life Technologies Corporation) supplemented with Gibco B-27 Supplements (Life Technologies Corporation), FGF (ProSpec-Tany TechnoGene Ltd., 20 ng/mL), and EGF (ProSpec-Tany TechnoGene Ltd., 20 ng/mL). LN229/GSCs were grown as spheres in flasks coated with Poly(2-hydroxyethyl methacrylate; Sigma-Aldrich Co. LLC).

Isolation and preparation of primary GBM cells and GSCs

The use of human GBM patient specimens has been approved by the Institutional Review Board at the Carilion Clinic. Freshly resected human GBM tumors (pathologically confirmed) were minced into small pieces. Single cells were prepared using the Papain cell dissociation system (Worthington Biochemical Corporation) or Liberase (Roche Diagnostics) according to manufacturer's instructions. Red blood cells were removed using the Red Blood Cell Lysis Solution purchased from Miltenyi Biotec Inc. Isolated cells were cultured in DMEM (Life Technologies Corporation) supplemented with 10% FBS (Atlas Biologicals, Inc.), streptomycin (100 μg/mL), penicillin (100 IU/ml), and 1× antibiotic-antimycotic (Life Technologies Corporation). Primary GBM cells were maintained at low passages.

GSCs were isolated and enriched using the sphere-formation assay. Primary GBM cells were cultured in stem cell culture media [DMEM or neurobasal media (Life Technologies Corporation) supplemented with B-27 supplement (Life Technologies Corporation), 20 ng/mL FGF-2 (Genscript), and 20 ng/mL EGF (Genscript)]. Isolated GSCs grew as spheres after 1 to 2 months of continuous culturing. GSCs were tested for their capability to self-renew using the sphere-formation assay described below.

Immunoblotting and quantification of band intensity

Immunoblotting was performed as described in our previous reports (11). In brief, cells were lysed and total protein was quantified using the Bradford assay (Bio-Rad Laboratories Inc.). An equal amount of total protein (20–25 μg) in each sample was loaded onto an SDS-PAGE gel. After transferring to PVDF membrane, the blot was incubated with antibodies. Antibodies were diluted as follows: anti-Cx43 (Sigma-Aldrich Co., 1:4000), anti-MGMT (Cell Signaling Technology, 1:300), anti–β-actin (Sigma-Aldrich Co. LLC, 1:10000), anti–phospho-AKT (Cell Signaling Technology, 1:1000), anti-AKT (Cell Signaling Technology, 1:1000), anti–phospho-AMPKα (Cell Signaling Technology, 1:1000), anti-AMPKα (Cell Signaling Technology, 1:1000), anti–phospho-MTOR (Cell Signaling Technology, 1:1000), anti-MTOR (Cell Signaling Technology, 1:1000), anti-GFAP (Cell Signaling Technology, 1:500), anti-NOTCH1 (Bio-Rad Laboratories Inc., 1:1000), and anti-GAPDH (Santa Cruz Biotechnology, Inc., 1:5000). Images were taken using a ChemiDoc MP System (Bio-Rad Laboratories Inc.). The intensity of the band was quantified using Image Lab software (Bio-Rad Laboratories Inc.) or ImageJ as described earlier (11). The relative level of Cx43 proteins (Cx43/ACTB) is defined as the ratio of band intensity of Cx43 to that of β-actin.

Viability assays

Viability assays were described previously (12). Cells (5×10^2 or 2.5×10^3) were plated in a 96-well plate or a 24-well plate, respectively. Cells were then treated with vehicle (DMSO), TMZ (25–400 μmol/L) once, αCT1 (50–100 μmol/L) every second day X 3 doses, or a combination of TMZ and αCT1. After one week, cell viability was monitored using the following assays: MTS or Trypan blue exclusion. In MTS assay, 10 μL MTS (Promega) was added to each well, then incubated at 37°C for 1 hour. The absorbance at 490 nm was measured using the FilterMax F3 microplate reader (Molecular Devices, LLC) according to the manufacturer's instructions. Percent cell viability was obtained by dividing the absorbance of treatment groups to those of untreated groups. In the Trypan blue exclusion assay, cells were trypsinized and stained with Trypan blue. Trypan blue-negative cells (viable) were counted using a hemocytometer. The percentage of viable cells was defined as the ratio of cell number in the treatment group to that of the control group. TMZ IC_{50}s were calculated using the GraphPad Prism software.

Kaplan–Meier analysis of The Cancer Genome Atlas gene expression data

Clinical variables of GBM patients, such as survival time and vital status, were retrieved from The Cancer Genome Atlas (TCGA) Data Portal (https://tcga-data.nci.nih.gov/tcga/). Gene expression data, including for GBM patients (AglientG450A_07; Aglient 244K custom gene expression and HuEx-1_0-st-v2; Affymetrix human exon 1.0 ST array), was downloaded from the Pan-cancer project (syn1461183) on Synapse (http://www.synapse.org). A cohort of 89 or 437 GBM patients was first divided into

A

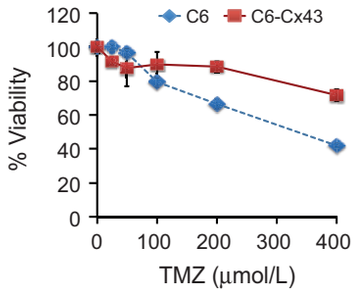

B

Cell lines	MGMT expression	Reference
SF-295	–	14
U87MG	–	12
A172	–	12
T98G	+	13
LN229	–	12
SF-268	–	12
U251	–	13
SNB-75	–	16
LN-18	+	15

C

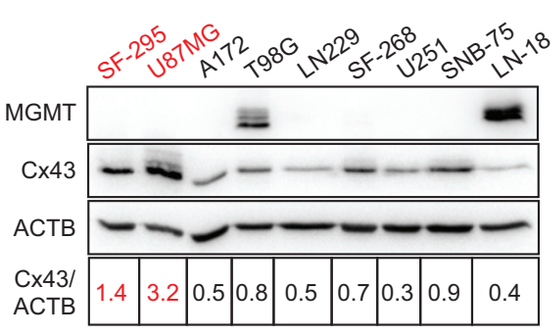

D

Cell lines	IC_{50} of TMZ (μmol/L)	Reference
SF-295	~500	14
U87MG	~1000	12
A172	~30	12
LN229	~20	12
SF-268	~20	12
U251	~20	13
SNB-75	No data	
T98G	~1000	13
LN-18	~800	15

E

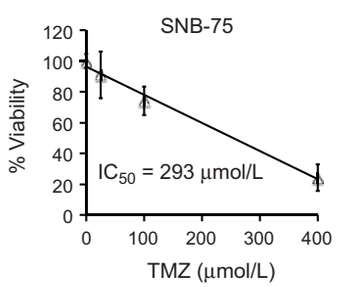

F

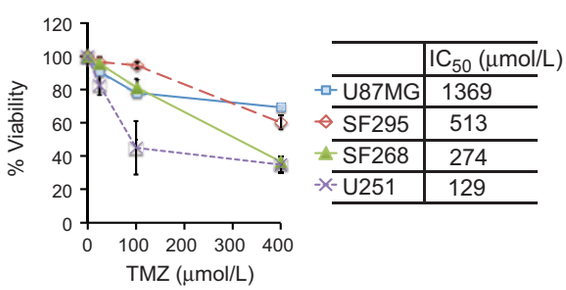

G

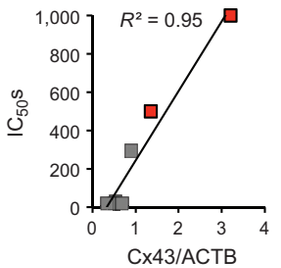

H

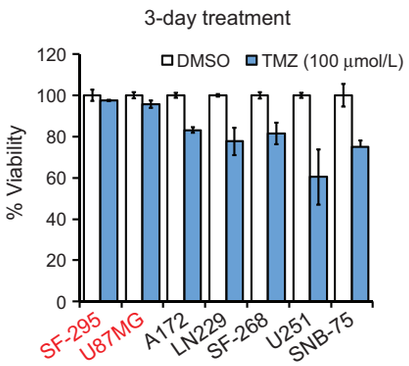

I

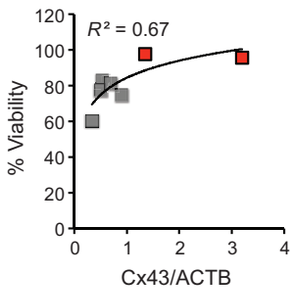

Figure 1.
Cx43 expression levels are inversely correlated with the TMZ sensitivity of GBM cell lines. A, TMZ sensitivity in rat glioma C6 and C6-Cx43 cells. B, MGMT status in GBM cell lines. C, expression of MGMT and Cx43 in nine GBM cell lines. β-Actin (ACTB) was the loading control. The ratio of the band intensity of Cx43 normalized to that of ACTB (Cx43/ACTB) is shown. Cells with highest levels of Cx43 are marked in red. D, published TMZ IC_{50}s. E, IC_{50} of TMZ in SNB-75 cells. F, TMZ IC_{50}s of U87MG, SF295, SF268, and U251 cells tested in our hands. G, correlation between IC_{50}s and Cx43 level. H, viability of MGMT-deficient GBM cells treated with 100 μmol/L of TMZ for 3 days. I, correlation between cell viability and Cx43 level. Error bar, SD from three independent experiments.

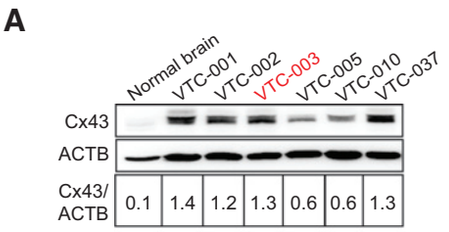

D

Tissues	Cx43 level	Number of cases
Cerebral cortex glia cells	Low	N/A
High-grade glioma	High	2
	Medium	2
	Low	1
	Not detected	3

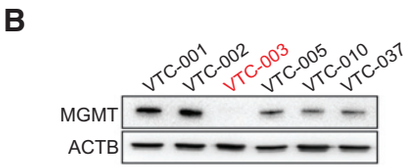

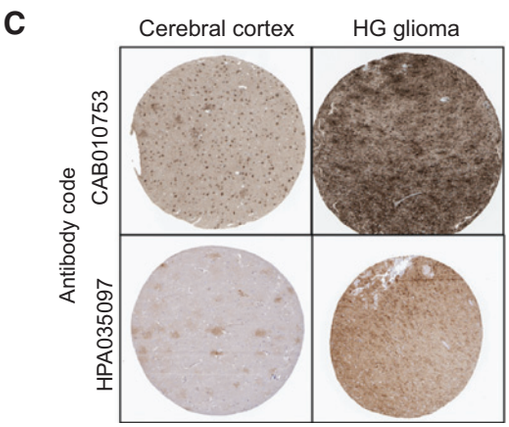

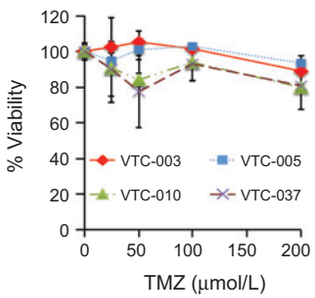

Figure 2.
Cx43 in primary GBM cells. A, expression of Cx43 in primary GBM cells. Cell lysate from normal brain – control. B, MGMT expression in primary GBM cells. C, representative IHC analysis results of Cx43 in high-grade glioma (data from the Human Protein Atlas). D, summary of IHC analysis of Cx43 expression. E, viability of primary GBM cells treated with TMZ at different doses.

$MGMT_{low}$ and $MGMT_{high}$ based on *MGMT* mRNA levels using mean *MGMT* mRNA levels of all the patients as the denominator. The same approach was used to further divide patients into $GJA1_{low}$ and $GJA1_{high}$ groups. Patients who survived for less than 5 days after diagnosis were considered outliers and excluded from this study. A Kaplan–Meier survival analysis was performed using the JMP software (SAS Institute Inc.).

Sphere-formation assay

Sphere-formation assays were performed as described earlier (13). Briefly, GSCs (50 cells per well) were plated in a 96-well plate. Cells were then treated as described above. Two to three weeks later, the numbers of wells with spheres were counted. The percentage of wells with spheres was defined as the ratio of wells with spheres to wells initially plated.

Cyto-ID fluorescence spectrophotometric assay

The Cyto-ID fluorescence spectrophotometric assay to measure autophagy has been described previously (12). In brief, cells were stained with Cyto-ID at 37°C for 30 minutes in the dark. The cells were then divided: one-half for the measurement of Cyto-ID; the other half for the MTS cell viability assay as described above. In some experiments, cell number was determined by the CellTiter-Blue assay (Promega) according to manufacturer's instructions. The Cyto-ID fluorescence was read at excitation 480 nm and emission 530 nm and the fluorescence intensity of CellTiter-Blue was read at excitation 560 nm and emission 590 nm using the FilterMax F3 microplate reader. Relative Cyto-ID fluorescence is defined as the ratio of the Cyto-ID reading to the MTS or CellTiter-Blue reading. Fold change in Cyto-ID fluorescence was defined as the ratio of relative Cyto-ID fluorescence in treated cells to that in control cells.

Caspase-3/7 activity assay

The caspase-3/7 activity assay has been described previously (13). In brief, cells were plated in a 96-well plate and treated with drugs as described above. The activity of caspase-3/7 was measured using the Caspase-Glo 3/7 assay (Promega) based on manufacturer's instructions. The fold change of caspase-3/7 activity was defined as the ratio of caspase-3/7 luminescence in the treated to that in control cells.

Mouse experiments

Mouse experiments were performed based on methods described previously, with modifications (12, 13). All animal studies were approved by the Institutional Animal Care and Use Committee of Virginia Tech. LN229/GCSs (1×10^5) were subcutaneously injected into BALB/c nude mice (Charles River Laboratories). After 14 days, mice were divided into four groups: (i) vehicle/control, (ii) TMZ alone, (iii) αCT1 alone,

and (iv) TMZ and αCT1. The treatment regimen was as follows: αCT1 peptide (100 mg/kg/day) was administered via intratumoral injection on days 1 and 2 then every second day thereafter. TMZ (7.5 mg/kg/day) was administered by intraperitoneal injection every second day starting on day 2. For the groups 1–3, the vehicle DMSO or 1× PBS was used accordingly. This treatment regimen continued for 2 weeks. The tumor sizes were measured every other day using a caliper. Tumor volume was calculated ((length × width^2)/2).

Statistical analyses

The Student *t* test and the one-way ANOVA with Tukey *post hoc* test for multiple comparisons were used for statistical analyses. These tests were done using the SPSS software.

Results

Cx43 expression level inversely correlates with TMZ sensitivity in MGMT-deficient GBM cells

How Cx43 governs TMZ resistance remains elusive. To further understand the mechanism of Cx43-mediated TMZ resistance, we first monitored the TMZ sensitivity of a rat malignant glioma cell line C6 that ectopically expresses Cx43. Consistent with previous reports (7, 8), C6 cells with exogenous Cx43 became resistant to TMZ (Fig. 1A). We then investigated the relationship between Cx43 expression and MGMT-independent TMZ resistance in human GBM cell lines. Previous studies had indicated that MGMT was expressed in the T98G or LN-18 cell lines only, but absent in SF295, U87MG, A172, LN229, SF-268, U251, and SNB-75 cells (Fig. 1B; refs. 14–18). We found that of the MGMT-negative GBM cell lines, Cx43 was highly expressed in SF295 and U87MG cells (highlighted in red, Fig. 1C). Intriguingly, the reported TMZ IC_{50}s of SF295 and U87MG cells was remarkably higher than those of the other GBM cell lines (Fig. 1D). As we could not find it documented in the literature, we assayed the TMZ IC_{50} of SNB75 cells and determined it to be 293 μmol/L (Fig. 1E). To validate TMZ sensitivities reported previously for other GBM cell lines, we treated U87MG, SF295, SF268, and U251 cells with different doses of TMZ. The IC_{50}s of above cell lines were 1369, 513, 274, and 129 μmol/L, respectively (Fig. 1F), Although SF268 and U251 cells were less sensitive to TMZ in our hands, the difference in TMZ responsiveness among these GBM cell lines was more or less in line with those measured by earlier workers (see Fig. 1 for these references). Regression analysis of Cx43 and TMZ IC_{50}s in MGMT-deficient cell lines demonstrated that there was a strong relationship between TMZ responsiveness and Cx43 levels (Fig. 1G; refs. 14–16). Consistent with this trend, the high Cx43-expressing lines SF295 and U87MG showed the lowest cytotoxicity when treated with 100 μmol/L of TMZ for 3 days (Fig. 1H) and there was a strong correlation between TMZ-induced reduction in cell viability and levels of Cx43 expressed (Fig. 1I).

We next examined Cx43 expression and TMZ responses in GBM primary cells from freshly resected patient tumors. The levels of Cx43 in all GBM patient samples were approximately 6- to 14-fold higher than that in the normal brain (Fig. 2A), consistent with the results from The Protein Atlas database (Fig. 2C and D). Among all six primary GBM cells, only VTC-003 cells expressed no MGMT (Fig. 2B). The ratio of Cx43 to ACTB in VTC-003 cells was equivalent to that in SF295 cells (Figs. 1C and 2A). As expected, VTC-003 exhibited significant resistance to TMZ (Fig. 2E) with an IC_{50} of approximately 3 mmol/L.

Cx43 expression level inversely correlates with the survival of MGMT-deficient GBM patients

Prompted by these results, we sought to determine whether Cx43 is a prognostic marker for MGMT-deficient GBM. We retrieved patient clinical information and corresponding gene expression results from the TCGA. Two datasets AglientG4502A_07 (cDNA microarray, 89 patients) and HuEx-

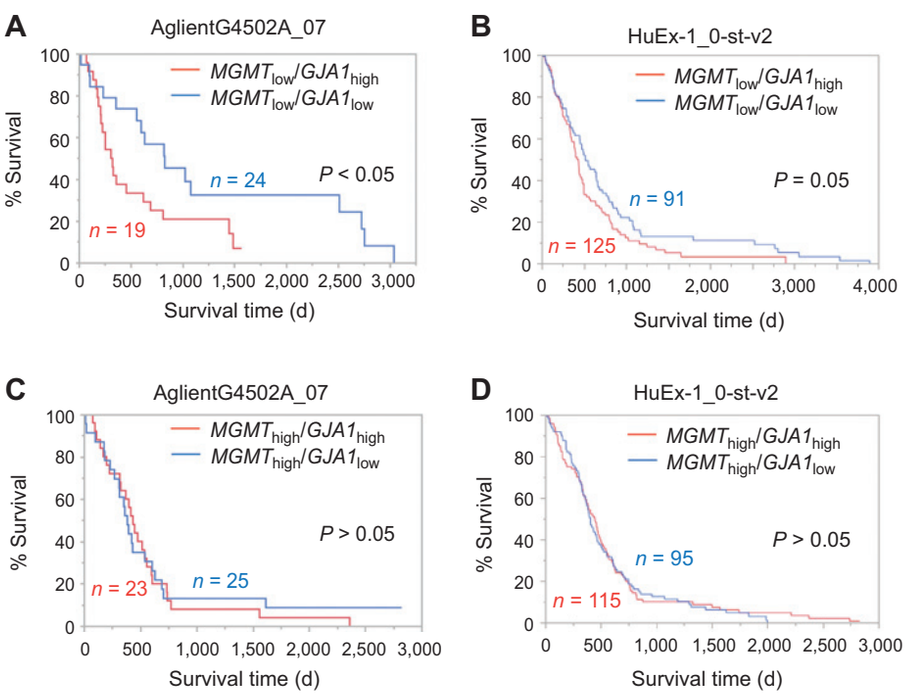

Figure 3.
Cx43 level inversely correlated with the survival of MGMT-deficient GBM patients. Kaplan–Meier survival analyses of $MGMT_{low}$ (A and B) and $MGMT_{high}$ (C and D) GBM patients. The survival time of GBM patients (*x*-axis) is defined as days after diagnosis. Gap junction protein A1 (GJA1) is the gene encoding Cx43. Two datasets (AglientG4502A_07 and HuEx-1_0-st-v2) retrieved from the TCGA were used.

1_0-st-v2 (Exon array, 437 patients) were used. We first divided patient samples from the TCGA database into two groups: $MGMT_{low}$ and $MGMT_{high}$ based on mRNA levels. In the $MGMT_{low}$ group, patients with high levels of *GJA1* mRNA ($GJA1_{high}$) had a significantly shorter life span than those with low levels of *GJA1* mRNA ($GJA1_{low}$; Fig. 3A and B, $P < \text{or} = 0.05$). In contrast, there was no significant difference between $GJA1_{high}$ and $GJA1_{low}$ patients in the $MGMT_{high}$ group (Fig. 3C and D; $P > 0.05$). These results strongly infer that Cx43 expression levels inversely correlate with the prognosis of MGMT-deficient GBM patients.

αCT1, a Cx43 mimetic peptide, sensitizes GBM cells to TMZ

αCT1 is a mimetic of the Cx43 CT (Fig. 4A) that selectively inhibits Cx43 hemichannel (HC) activity via a mechanism involving a competitive interaction with ZO-1 (zonula occludens-1)—a PDZ (Post synaptic density, Disks-large, Zonula occludens-1)–containing protein (9). In light of recent findings that Cx43 CT may control TMZ drug resistance (7, 8), we sought to determine whether αCT1 restored drug sensitivity in MGMT-deficient GBM cells. Tumor cells were treated with αCT1, TMZ, or a combination of both these drugs. In $MGMT_{deficient}$ and $Cx43_{high}$ cells including

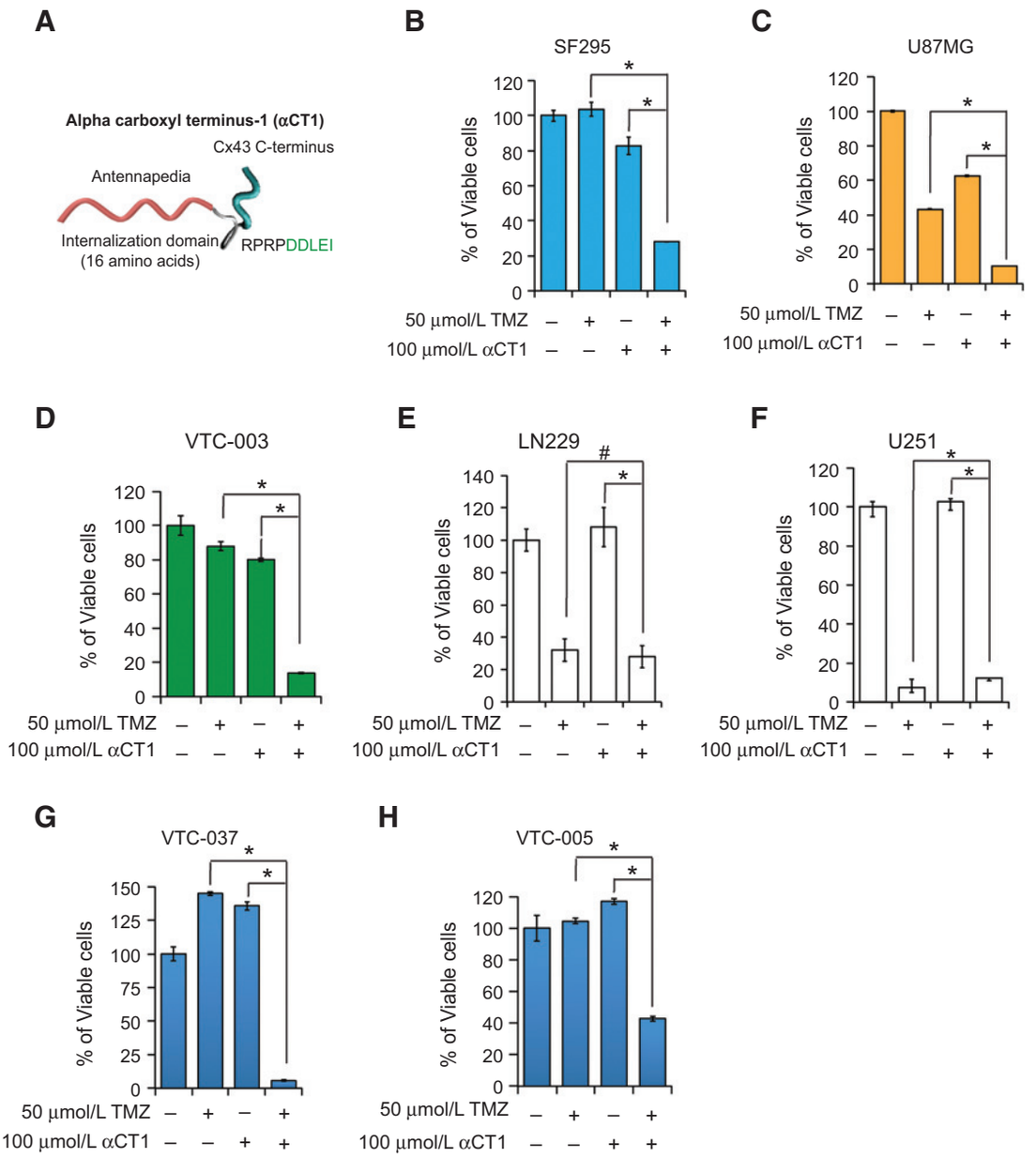

Figure 4.
αCT1 sensitizes GBM cells to TMZ. A, αCT1 peptide is composed of an antennapedia cell internalization domain and nine amino acids at the CT of Cx43 (i.e., RPRPDDLEI). Viability of SF295 (B), U87MG, (C), VTC-003 (D), LN229 (E), U251 (F), VTC-037 (G), and VTC-005 (H) cells treated with αCT1 and/or TMZ for 1–2 weeks. Error bar, SD from experiments performed in triplicate. *, $P < 0.05$ and #, $P > 0.05$.

SF-295, U87MG, and VTC-003, the combination of αCT1 and TMZ resulted in a marked and synergistic reduction of cell viability compared with each treatment alone (Fig. 4B–D). In contrast, the combinational treatment failed to significantly induce a synergistic growth inhibition in $MGMT_{deficient}$ and $Cx43_{low}$ LN229 (Fig. 4E) or U251 (Fig. 4F) cells. Primary GBM cells VTC-037 and VTC-005 that expressed low levels of MGMT (Fig. 2B) also responded to the combination of αCT1 and TMZ (Fig. 4G and H). VTC-005 cells express 2-fold lower levels of Cx43 than VTC-037 (Fig. 2A). Intriguingly, the response of VTC-005 cells to TMZ was also less efficient than that of VTC-037. Together, our results indicate that inhibition of Cx43 channels substantially reduced TMZ resistance in MGMT-deficient GBM cells and that this effect was strongly related to the level of Cx43 expressed by patient cells.

Glioblastoma stem cells express high levels of Cx43 and are resistant to TMZ

Because GSCs are highly tumorigenic, it has been suggested that GSCs are the prime cause of GBM tumor recurrence (19). Thus, targeting GSCs is an appealing therapeutic approach for GBM. GSCs are also resistant to current therapies including TMZ (20). Although this resistance may involve different mechanisms, we postulated that Cx43 might also render GSCs resistant to TMZ. To test this, we isolated and enriched GSCs from LN229 cells (LN229/GSC). Compared with parental LN229 cells, LN229/GSCs showed a loss of GFAP (Glial Fibrillary Acidic Protein, an astrocyte marker) and enrichment of the GSC marker NOTCH1 (Notch homolog 1; Fig. 5A; ref. 21). Notably, the level of Cx43 was increased in LN229/GSCs compared with the parental LN229 line (Fig. 5B). We further confirmed that another TMZ-resistant GSC line GS9-6/NOTCH1+ (Fig. 5C; refs. 21, 22) also expressed elevated levels of Cx43 (Fig. 5B). Both LN229/GSC and GS9-6/NOTCH1+ stem cell lines were also found to be MGMT deficient (Fig. 5B). In addition, we isolated and enriched GSC lines VTC-036/GSC, VTC-061/GSC, and VTC-064/GSC directly from freshly resected human GBM patient tissues. We found that an MGMT-negative VTC-064/GSC line expressed a high level of Cx43 (Fig. 5C and D), equivalent to that of LN229/GSCs (Fig. 5B). We next determined the sensitivity of these GSCs to TMZ. Compared with the parental LN229 cells, LN229/GSCs were significantly less sensitive to TMZ (Fig. 5F, 8.3% vs. 46.3%).

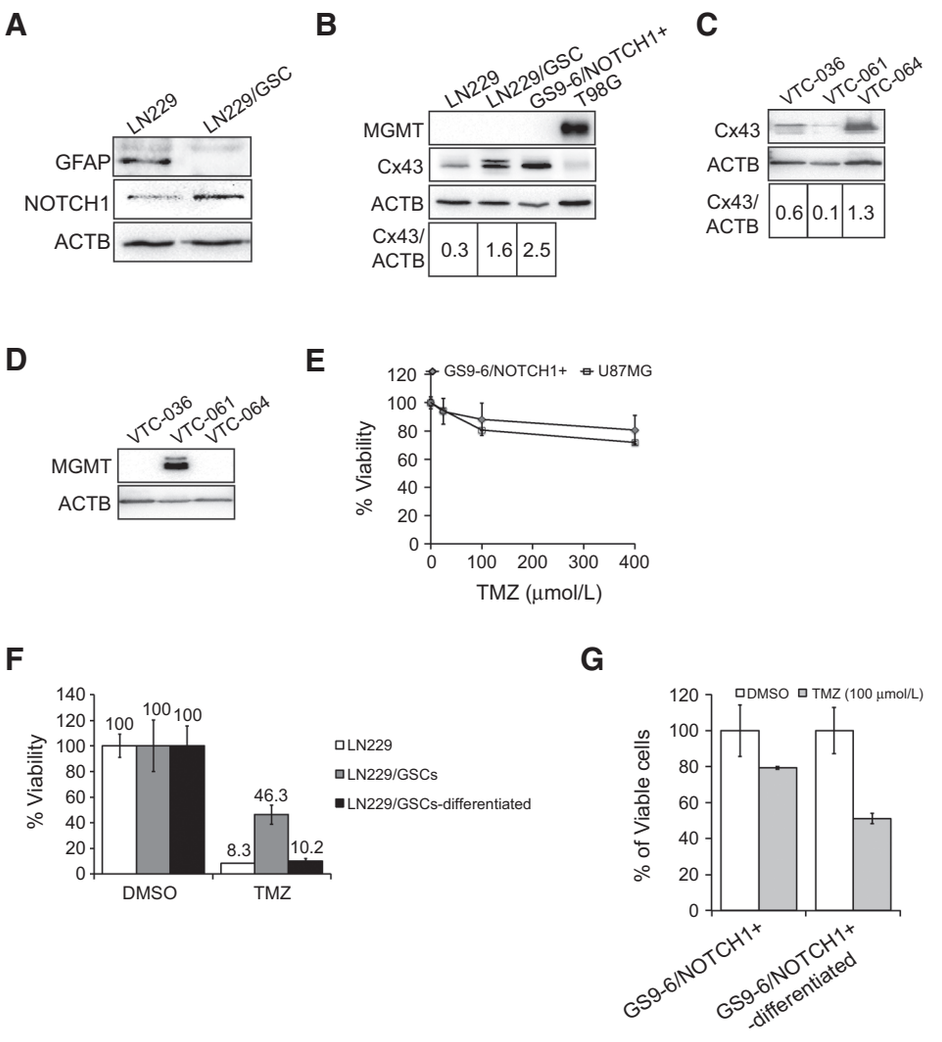

Figure 5.
Cx43 is enriched in TMZ-resistant GSCs. A, expression of GFAP and NOTCH1 in LN229 and LN229/GSC. B, expression of MGMT and Cx43 in GSCs. C, expression of Cx43 in GSC lines VTC-036/GSC, VTC-061/GSC, and VTC-064/GSC. D, expression of MGMT in above GSCs. E, sensitivity of GS9-6/NOTCH1+ cells to TMZ. F, viability of LN229/GSCs and differentiated tumor cells treated with TMZ. G, viability of GS9-6/NOTCH1+ and differentiated tumor cells treated with TMZ. Error bar, SD from experiments performed in triplicate.

GS9-6/NOTCH1+ cells also proved resistant to TMZ, displaying drug sensitivity equivalent to the TMZ-resistant U87MG cell line (Fig. 5E). Importantly, differentiation of LN229/GSCs or GSC9-6/NOTCH1+ cells into mature GBM lineages resulted in a rescue of TMZ sensitivity (Fig. 5F and G). Taken together, these data indicated that GSCs express high levels of Cx43 and are resistant to TMZ.

αCT1 sensitizes GSCs to TMZ

We then asked whether αCT1 restores GSCs' sensitivity to TMZ. As expected, the combination of αCT1 and TMZ, but neither treatment alone, blocked the sphere formation of GS9-6/NOTCH1+ cells (Fig. 6A and B), LN229/GSCs (Fig. 6C), and VTC-064/GSCs (Fig. 6D). The cell viability of LN229/GSCs was also significantly reduced by the combinational αCT1/TMZ treatment (Fig. 6E). Furthermore, αCT1 and TMZ (red line) together substantially blocked the growth of human-derived LN229/GSC tumors in mice (Fig. 6F). These data indicate that αCT1 circumvents TMZ resistance of GSCs both *in vitro* and *in vivo*.

αCT1 blocks the AKT/AMPK/MTOR signaling pathway and induces autophagy and apoptosis

Connexin HC activity has been shown to be critical for the activation of AKT/AMPK/MTOR signaling pathway (23). In this pathway, AKT (protein kinase B) suppresses AMPK (AMP-activated protein kinase) and, in turn, blocks the inhibition of MTOR by AMPK, leading to MTOR activation. As αCT1 selectively inhibits the activity of Cx43 HCs (24), we hypothesized that this peptide targeted the AKT/AMPK/MTOR signaling pathway. In the nine GBM cell lines, AKT and MTOR were active in the high Cx43-expressing SF295 and U87MG, but not in the other GBM lines, coinciding with inactivation of AMPKα (an active subunit of AMPK complex; Fig. 7A). To compare the effect of αCT1 on AKT/AMPK/MTOR signaling pathway in cells with different levels of Cx43 and responsiveness to TMZ, we treated LN229 ($Cx43_{low}$/$TMZ_{sensitive}$) and LN229/GSCs ($Cx43_{high}$/$TMZ_{resistant}$) with αCT1 and/or TMZ. Although αCT1 alone blocked AKT, activated AMPKα, and inactivated MTOR in LN229/GSCs, it did not do so in parental LN229 cells (Fig. 7B). Of note, TMZ alone had no

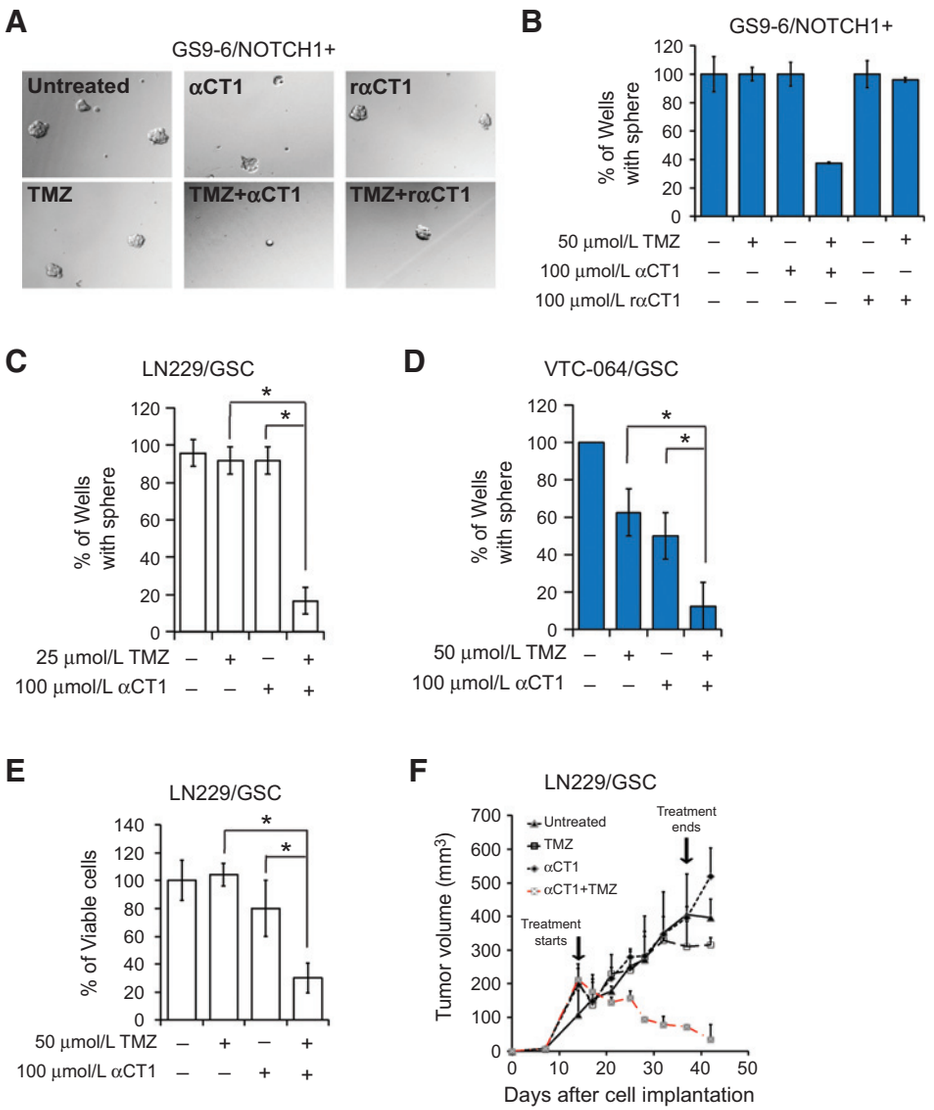

Figure 6.
αCT1 sensitizes GSCs to TMZ. A, images of GS9-6/NOTCH1+ spheres treated with αCT1 and/or TMZ. rαCT1 is an inactive form of αCT1 with a reversed sequence of Cx43 CT amino acids (i.e., ielddprpr). B, sphere formation of GS9-6/NOTCH1+. C, sphere formation of LN229/GSCs. D, sphere formation of VTC-064/GSC. E, viability of LN229/GSCs. F, growth curve of LN229/GSC tumors in mice. Error bar, SD from experiments performed in triplicate. *, $P < 0.05$.

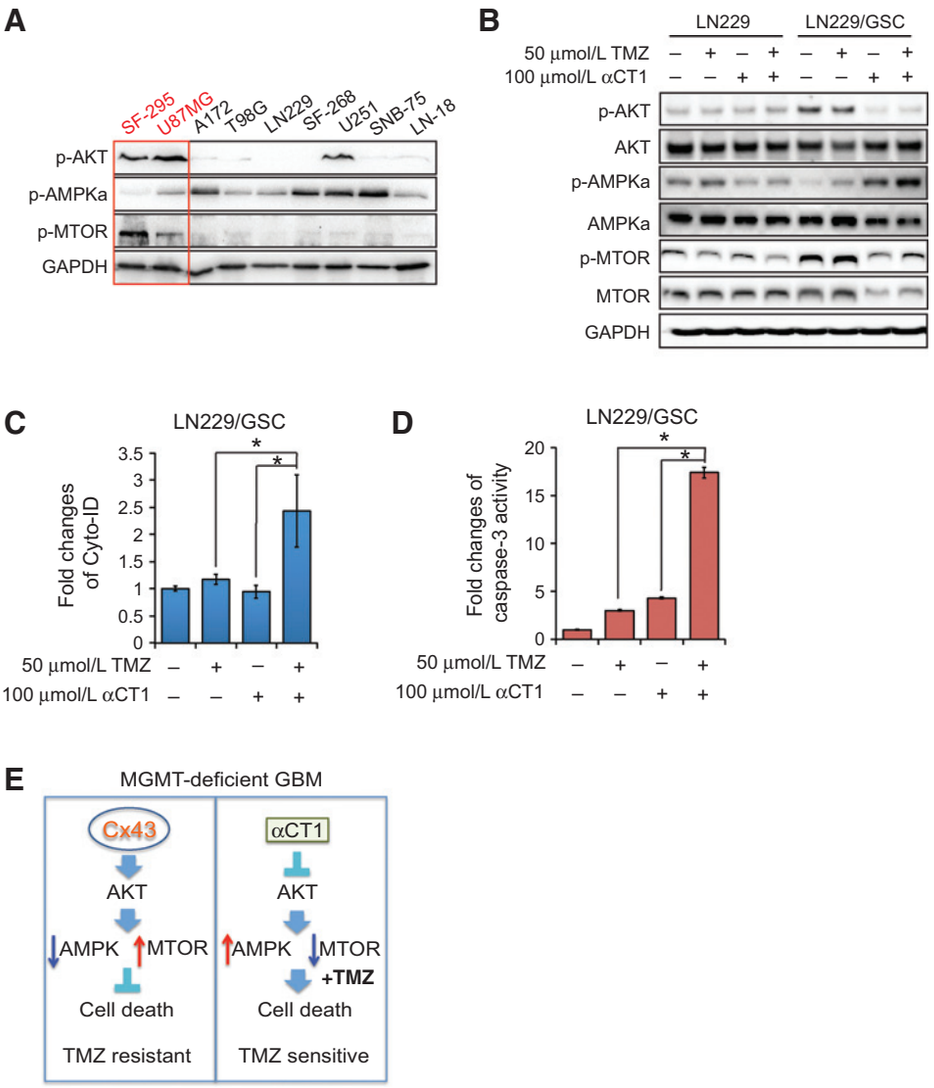

Figure 7.
The αCT1 and TMZ combinational treatment suppresses the AKT/AMPK/MTOR signaling pathway and synergistically induces autophagy and apoptosis. A, activity of AKT, AMPK, and MTOR in nine GBM cells lines. B, activity of AKT, AMPK, and MTOR in LN229 and LN229/GSCs treated with αCT1 and/or TMZ. C, autophagy assay in LN229/GSCs treated with TMA and/or αCT1. D, apoptosis assay. E, a model of MGMT-independent TMZ resistance and the mode of action of αCT1. Error bar, SD from experiments performed in triplicate. *, $P < 0.05$.

influence on this signaling pathway, suggesting that the inactivation of AKT/AMPK/MTOR signaling pathway by αCT1 may sensitize GBM cells to TMZ-induced growth inhibition. Given the important role of AKT/MTOR in autophagy and apoptosis, we hypothesized that the combination of αCT1 and TMZ synergistically activated autophagy and/or apoptosis. Consistent with this, it was determined that cotreatment of LN229/GSCs with αCT1 and TMZ synergistically induced autophagy (Fig. 7C) and apoptosis (Fig. 7D). Collectively, these results demonstrate that αCT1 blocks the AKT/AMPK/MTOR signaling pathway and induces autophagy and apoptosis.

Discussion

A novel paradigm is proposed for development of resistance of MGMT-deficient GBM patients to TMZ (Fig. 7E). In MGMT-deficient GBM cells, Cx43 activates AKT followed by inactivation of AMPK and activation of MTOR signaling. This leads to suppression of cell death. Thus, these MGMT-deficient GBM cells are TMZ resistant. On the other hand, αCT1, a selective inhibitor of Cx43 channel activity, blunts this process, and sensitizes MGMT-deficient GBM cells to TMZ-induced cell death. Hence, these MGMT-deficient GBM cells become sensitive to TMZ. This new paradigm demonstrates the potentially important role of Cx43 in sensitivity to the anticancer drug TMZ. Our results presented herein also offer possible options for the diagnosis and treatment of TMZ-resistant GBM.

The results shown in Fig. 3 demonstrate that Cx43 is an adverse prognostic marker for MGMT-deficient GBM. Our further work, presented in Figs. 4 and 5, reveals an important role of Cx43 in TMZ resistance in MGMT-deficient GBM cells. The reciprocal expression pattern of Cx43 and MGMT in GBM cells as well as the resensitization of GBM cells to TMZ by a Cx43 inhibitor strongly suggest that a high level of Cx43 contributes to MGMT-independent TMZ resistance. MGMT repairs DNA damage caused by TMZ; however, GBM patients with no or low levels of MGMT still become tolerant to TMZ (4). Thus, our work identifies a novel mechanism underlying TMZ resistance in MGMT-deficient GBM patients. The molecular pathway presented in Fig. 7E, left, further explains how Cx43 renders MGMT-deficient GBM

patients TMZ resistance. Taken together, our findings are of potential significance as they indicate path to new therapies involving the targeting of Cx43 that could be applied to MGMT-deficient/Cx43-high GBM patients.

Our results demonstrate that the combination of αCT1 and TMZ likely induces cell death through attenuating the activity of AKT/MTOR signaling pathway. However, the specific mechanism by which αCT1 acts on this signaling pathway remains to be elucidated. It has been recently determined that a prime site of action of αCT1 is in the perinexus, where the peptide uncoupled Cx43 from ZO-1 and prompted transition of undocked HCs into the gap junction (GJ; ref. 24). The sequestration of HCs into GJs induced by αCT1 resulted in decreased in HC activity, while maintaining GJ coupling. The mechanistic ability to selectively inhibit HC activity, without decreasing GJ coupling represents an important difference between αCT1 and other blockers of Cx43 function. This includes Cx43 antisense and the widely used Gap26 and Gap27 peptides, mimetics of the Cx43 extracellular loop domain, all of which inhibit Cx43 HC and GJ channel functions indiscriminately (25, 26). The targeted action of αCT1 on HCs may explain the altered activity of AKT/MTOR signaling, as HCs in normal or malignant glial cells provide pathways for escalated release of ATP and glutamate (27, 28). Glutamate exhibits its progrowth activity through activating the downstream signaling pathways such as PI3K or MAPK, both of which have been implicated in GBM pathogenesis (28).

Inhibition of Cx43 channel activity by αCT1 was found to enhance healing rates of two chronic wound types, diabetic foot and venous leg ulcers (10). Specifically, in multicenter phase II testing involving more than 250 patients, αCT1 significantly increased healing rates halving the time-to-closure of both chronic wound types (10). These clinical tests represented the first reports of a randomized trial of a connexin-targeting therapeutic in humans. Importantly with respect to the current study, no adverse events were associated with repeated exposure to αCT1 over the 12-week time course of either the venous leg or diabetic foot ulcer trials, including no detection of antibodies against αCT1 in patient sera (10). The safety of Cx43 antisense, Gap26/27 peptides or other nonselective approaches, which nonselectively block both HC and GJ functions of Cx43, has yet to be determined in humans. The preclinical studies shown in this report and the fact that αCT1 has been used in clinical trials for human patients with chronic wounds highlight the importance of the potential clinical application of αCT1 and TMZ combination for GBM patients, based on our finding that αCT1 sensitizes GBM cells to TMZ.

Our findings also have implications in treating other cancers, as TMZ has been used as a single agent or in combination with other cancer treatments in different types of cancer including pediatric solid tumors (i.e., medulloblastoma, neuroblastoma, Ewing sarcoma, hepatocarcinoma, etc.) and brain metastases from breast or lung cancer (29, 30). There are several ongoing clinical trials in which TMZ is used as a single agent to treat melanoma (31) and small cell lung cancer (32). Hence, a combined TMZ and Cx43 inhibitory treatment could provide a new and effective therapy for GBM and other cancers.

Disclosure of Potential Conflicts of Interest

J. Jourdan has ownership interest (including patents) in First String Research. R.G. Gourdie has ownership interest (including patents) in and is a consultant/advisory board member for First String Research Inc. No potential conflicts of interest were disclosed by the other authors.

Authors' Contributions

Conception and design: S.F. Murphy, Z. Sheng, P. Kanabur, R.G. Gourdie
Development of methodology: Z. Sheng, S. Guo, K.J. Pridham, P. Kanabur, R.G. Gourdie
Acquisition of data (provided animals, acquired and managed patients, provided facilities, etc.): S.F. Murphy, Z. Sheng, R.T. Varghese, S. Lamouille, S. Guo, P. Kanabur, A.M. Osimani, S. Sharma, C.M. Rodgers, G.R. Simonds
Analysis and interpretation of data (e.g., statistical analysis, biostatistics, computational analysis): S.F. Murphy, Z. Sheng, R.T. Varghese, S. Guo, P. Kanabur, A.M. Osimani, R.G. Gourdie
Writing, review, and/or revision of the manuscript: S.F. Murphy, Z. Sheng, S. Guo, R.G. Gourdie
Administrative, technical, or material support (i.e., reporting or organizing data, constructing databases): Z. Sheng, R.T. Varghese, S. Guo, J. Jourdan, C.M. Rodgers
Study supervision: Z. Sheng, R.G. Gourdie

Acknowledgments

The authors thank all of the members of the Sheng and Gourdie's laboratories for advice and guidance of this project. The authors also thank the patients with glioblastoma for their donation of tissue samples for our research.

Grant Support

This work was supported by the start-up fund from VTCRI and the research grant from The Elsa U. Pardee Foundation to Z. Sheng, the U.S. NIH grant RO1 HL56728 and the VBHRC grant to R.G. Gourdie, and a Virginia Center for Innovative Technology (CIT) grant to Z. Sheng and R.G. Gourdie.

The costs of publication of this article were defrayed in part by the payment of page charges. This article must therefore be hereby marked *advertisement* in accordance with 18 U.S.C. Section 1734 solely to indicate this fact.

Received May 13, 2015; revised September 11, 2015; accepted October 4, 2015; published OnlineFirst November 5, 2015.

References

1. Siegel R, Naishadham D, Jemal A. Cancer statistics, 2013. CA Cancer J Clin 2013;63:11–30.
2. Stupp R, Mason WP, van den Bent MJ, Weller M, Fisher B, Taphoorn MJ, et al. Radiotherapy plus concomitant and adjuvant temozolomide for glioblastoma. N Engl J Med 2005;352:987–96.
3. Grossman SA, Ye X, Piantadosi S, Desideri S, Nabors LB, Rosenfeld M, et al. Survival of patients with newly diagnosed glioblastoma treated with radiation and temozolomide in research studies in the United States. Clin Cancer Res 2010;16:2443–9.
4. Stupp R, Hegi ME, Mason WP, van den Bent MJ, Taphoorn MJ, Janzer RC, et al. Effects of radiotherapy with concomitant and adjuvant temozolomide versus radiotherapy alone on survival in glioblastoma in a randomised phase III study: 5-year analysis of the EORTC-NCIC trial. Lancet Oncol 2009;10:459–66.
5. Chen W, Wang D, Du X, He Y, Chen S, Shao Q, et al. Glioma cells escaped from cytotoxicity of temozolomide and vincristine by communicating with human astrocytes. Med Oncol 2015;32:43.
6. Yusubalieva GM, Baklaushev VP, Gurina OI, Zorkina YA, Gubskii IL, Kobyakov GL, et al. Treatment of poorly differentiated glioma using a combination of monoclonal antibodies to extracellular connexin-43 fragment, temozolomide, and radiotherapy. Bull Exp Biol Med 2014;157:510–5.
7. Munoz JL, Rodriguez-Cruz V, Greco SJ, Ramkissoon SH, Ligon KL, Rameshwar P. Temozolomide resistance in glioblastoma cells occurs partly through epidermal growth factor receptor-mediated induction of connexin 43. Cell Death Dis 2014;5:e1145.
8. Gielen PR, Aftab Q, Ma N, Chen VC, Hong X, Lozinsky S, et al. Connexin43 confers Temozolomide resistance in human glioma cells by modulating

the mitochondrial apoptosis pathway. Neuropharmacology 2013;75: 539–48.
9. Hunter AW, Barker RJ, Zhu C, Gourdie RG. Zonula occludens-1 alters connexin43 gap junction size and organization by influencing channel accretion. Mol Biol Cell 2005;16:5686–98.
10. Ghatnekar GS, Grek CL, Armstrong DG, Desai SC, Gourdie RG. The effect of a connexin43-based Peptide on the healing of chronic venous leg ulcers: a multicenter, randomized trial. J Invest Dermatol 2015; 135:289–98.
11. Sheng Z, Wang SZ, Green MR. Transcription and signalling pathways involved in BCR-ABL-mediated misregulation of 24p3 and 24p3R. EMBO J 2009;28:866–76.
12. Guo S, Liang Y, Murphy SF, Huang A, Shen H, Sobrado P, et al. A rapid and high content assay that quantitatively mesures autophagy and autophagy flux with potential clincal applications. Autophagy 2015; 11:560–72.
13. Sheng Z, Li L, Zhu LJ, Smith TW, Demers A, Ross AH, et al. A genome-wide RNA interference screen reveals an essential CREB3L2-ATF5-MCL1 survival pathway in malignant glioma with therapeutic implications. Nat Med 2010;16:671–7.
14. Gaspar N, Marshall L, Perryman L, Bax DA, Little SE, Viana-Pereira M, et al. MGMT-independent temozolomide resistance in pediatric glioblastoma cells associated with a PI3-kinase-mediated HOX/stem cell gene signature. Cancer Res 2010;70:9243–52.
15. Yoshino A, Ogino A, Yachi K, Ohta T, Fukushima T, Watanabe T, et al. Effect of IFN-beta on human glioma cell lines with temozolomide resistance. Int J Oncol 2009;35:139–48.
16. Qiu ZK, Shen D, Chen YS, Yang QY, Guo CC, Feng BH, et al. Enhanced MGMT expression contributes to temozolomide resistance in glioma stem-like cells. Chinese J Cancer 2014;33:115–22.
17. Fukai J, Koizumi F, Nakao N. Enhanced anti-tumor effect of zoledronic acid combined with temozolomide against human malignant glioma cell expressing O6-methylguanine DNA methyltransferase. PLoS ONE 2014;9:e104538.
18. Chen ZP, Wang ZM, Carter CA, Alley MC, Mohr G, Panasci LC. Both extraneuronal monoamine transporter and O(6)-methylguanine-DNA methyltransferase expression influence the antitumor efficacy of 2-chloroethyl-3-sarcosinamide- 1-nitrosourea in human tumor xenografts. J Pharmacol Exp Ther 2001;296:712–5.
19. Yan K, Yang K, Rich JN. The evolving landscape of glioblastoma stem cells. Curr Opin Neurol 2013;26:701–7.
20. Beier D, Schulz JB, Beier CP. Chemoresistance of glioblastoma cancer stem cells–much more complex than expected. Mol Cancer 2011;10:128.
21. Pohlmann ES, Patel K, Guo S, Dukes MJ, Sheng Z, Kelly DF. Real-time visualization of nanoparticles interacting with glioblastoma stem cells. Nano Lett 2015;15:2329–35.
22. Gilbert CA, Daou MC, Moser RP, Ross AH. Gamma-secretase inhibitors enhance temozolomide treatment of human gliomas by inhibiting neurosphere repopulation and xenograft recurrence. Cancer Res 2010;70: 6870–9.
23. Chi Y, Gao K, Li K, Nakajima S, Kira S, Takeda M, et al. Purinergic control of AMPK activation by ATP released through connexin 43 hemichannels - pivotal roles in hemichannel-mediated cell injury. J Cell Sci 2014; 127:1487–99.
24. Rhett JM, Jourdan J, Gourdie RG. Connexin 43 connexon to gap junction transition is regulated by zonula occludens-1. Mol Biol Cell 2011;22: 1516–28.
25. Desplantez T, Verma V, Leybaert L, Evans WH, Weingart R. Gap26, a connexin mimetic peptide, inhibits currents carried by connexin43 hemichannels and gap junction channels. Pharmacol Res 2012;65:546–52.
26. Pollok S, Pfeiffer AC, Lobmann R, Wright CS, Moll I, Martin PE, et al. Connexin 43 mimetic peptide Gap27 reveals potential differences in the role of Cx43 in wound repair between diabetic and non-diabetic cells. J Cell Mol Med 2011;15:861–73.
27. Orellana JA, Froger N, Ezan P, Jiang JX, Bennett MV, Naus CC, et al. ATP and glutamate released via astroglial connexin 43 hemichannels mediate neuronal death through activation of pannexin 1 hemichannels. J Neurochem 2011;118:826–40.
28. Lyons SA, Chung WJ, Weaver AK, Ogunrinu T, Sontheimer H. Autocrine glutamate signaling promotes glioma cell invasion. Cancer Res 2007; 67:9463–71.
29. De Sio L, Milano GM, Castellano A, Jenkner A, Fidani P, Dominici C, et al. Temozolomide in resistant or relapsed pediatric solid tumors. Pediatric Blood Cancer 2006;47:30–6.
30. Tatar Z, Thivat E, Planchat E, Gimbergues P, Gadea E, Abrial C, et al. Temozolomide and unusual indications: review of literature. Cancer Treat Rev 2013;39:125–35.
31. Beasley GM, Speicher P, Augustine CK, Dolber PC, Peterson BL, Sharma K, et al. A multicenter phase I dose escalation trial to evaluate safety and tolerability of intra-arterial temozolomide for patients with advanced extremity melanoma using normothermic isolated limb infusion. Ann Surg Oncol 2015;22:287–94.
32. Zauderer MG, Drilon A, Kadota K, Huberman K, Sima CS, Bergagnini I, et al. Trial of a 5-day dosing regimen of temozolomide in patients with relapsed small cell lung cancers with assessment of methylguanine-DNA methyltransferase. Lung Cancer 2014;86:237–40.